Available online at www.sciencedirect.com
SCIENCE DIRECT®
Journal of Sound and Vibration 284 (2005) 783–803
JOURNAL OF SOUND AND VIBRATION
www.elsevier.com/locate/jsvi

The critical phenomena in a hysteretic model due to the interaction between hysteretic damping and external force

Z. Chen[a], Z.Q. Wu[a,b], P. Yu[a,*]

[a]*Department of Applied Mathematics, The University of Western Ontario, London, Ont., Canada N6A 5B7*
[b]*Department of Mechanics, Tianjin University, Tianjin, 300072, P.R. China*

Received 20 August 2003; received in revised form 6 July 2004; accepted 15 July 2004
Available online 21 November 2004

Abstract

A self-excited system involving a van der Pol-type damping and a hysteretic damper representing restoring force is investigated in this paper. The influence of external force on the dynamic behavior of the hysteretic system is analyzed in detail. Numerical simulations show that, under an external force, the original hysteretic system can exhibit the so-called *critical phenomena*, where the hysteretic resorting force of the system may no longer obey the traditional piecewise function form. This new finding reveals that the system's behavior changes dramatically when an external force is present. Modified bilinear force paths are proposed to accommodate the new phenomena. It is shown that a hysteretic system can exhibit more complex dynamical behavior when an external forcing is applied, and that the critical phenomena may exist even when the system reaches its steady state. A study is presented on the necessary condition for the existence of the critical phenomena. More interestingly, it has been found that the hysteretic forcing can suppress chaotic motions, suggesting an alternative approach to control chaos.

1. Introduction

Hysteretic systems feature a special input–output relationship. If a system has a lag in the output with regard to the input, or the output depends on the input, then the system is said

*Corresponding author. Fax: +1 519 661 3523.
E-mail address: pyu@pyu1.apmaths.uwo.ca (P. Yu).

0022-460X/$ - see front matter © 2004 Elsevier Ltd. All rights reserved.
doi:10.1016/j.jsv.2004.07.018

to be endowed with hysteresis. Physical systems with hysteresis have several applications in different areas, such as mechanical engineering [1,2], structure engineering [3,4], smart material [5–7] and other fields of science and engineering [8,9], to mention only a few. Various models of hysteresis have been proposed in the past two decades. For example, the Ramberg–Osgood equation has been widely used to describe stress–strain hysteresis in many materials [4], Bouc–Wen models are very popular in the study of structural mechanics [10], and the bilinear hysteretic loop is usually the most practical approximation in many applications [3,11,12]. Recently, researchers have paid attention to self-excited systems with hysteresis which often appear in engineering systems. Dowell [13] proposed an airfoil with hysteretic nonlinearity in modelling supersonic flutter. Ding et al. [11] studied the instability and bifurcations of a self-excited hysteretic system using the average method and singularity theory. Wu et al. [12] investigated the same system considered in Ref. [11] without external forcing and used the singularity theory to obtain new transition varieties and new bifurcation solutions.

A common feature in the bilinear hysteretic loop, described by Ding et al. [11] and Wu et al. [12], is that the routes of the restoring force do not change their directions along the two horizontal paths in the first half of the lines (see Fig. 2 in the next section). That is, the hysteretic paths follow the Masing rules. (For a general discussion of Masing rules, see Refs. [9,10].) However, we have found from numerical simulations that this is not always true [14]. Since the motion of the system may change its direction at any point on the two horizontal paths where the velocity of the motion reaches zero, complicated characteristics of the hysteretic forcing can be exhibited, which have not been observed in the traditional behavior of such systems. Such a point (at which the velocity of motion is zero) is called the *critical turning point* [15]. We call such a situation the *critical phenomenon*. This phenomenon has been observed before [3,9,15], but has not been studied in detail. In this paper, with the aid of numerical simulations, we shall use spectral analysis to show that a necessary condition, for a hysteretic system to exhibit the critical phenomenon, is the existence of at least two modes in the system which are in competition [16].

In this paper, the same self-excited hysteretic model studied by Ding et al. [11] and Wu et al. [12] will be re-investigated. It is shown that the external force may complicate the dynamical behavior of the system and, thereafter, critical phenomena may occur. These bilinear hysteretic force paths when external force exists are inconsistent with the original hysteretic model [11]. Thus, revised hysteretic force paths are proposed to model the critical phenomena when an external force is present (see Fig. 3). However, it has recently been found that the critical phenomena described by Chen et al. [14] can also be observed in steady states of the hysteretic system. Moreover, numerical studies indicate that the hysteretic force can suppress the chaotic motions of the driven van der Pol oscillator, suggesting that hysteretic force may be used in controlling chaos.

The rest of the paper is organized as follows. For convenience and completeness, the hysteretic system studied in this paper is described in the next section. In Section 3, the influence of the external force on the dynamical behavior of the hysteretic system is investigated. Then, in Section 4, the critical phenomena appearing in the steady states of the system are discussed in detail. Chaos control of the van der Pol system using hysteretic force is given in Section 5. Finally, conclusions are drawn in Section 6.

2. A self-excited hysteretic system

The nonlinear mechanical system, with a van der Pol-type damping, a hysteretic damper and an external force, is shown in Fig. 1. Ding et al. [11] and Wu et al. [12] have investigated the behavior of this system using the singularity theory of bifurcations. For convenience and completeness, we briefly describe the model below. The mass, m, is attached to a van der Pol-type negative damping and a hysteretic damper, where $F(x)$ is the hysteretic restoring force and x is the displacement of the mass.

The dimensionless governing equation describing the motion of the mechanical system is given by the following equation [11] (for convenience, the same notations, x, $F(x)$ and $f(t)$ are used):

$$\ddot{x} + x - (\beta - x^2)\dot{x} + F(x) = f(t), \tag{1}$$

where $f(t) = K\cos\Omega t$ (the unit of Ω is Hz), representing the external force and β is the van der Pol damping coefficient. The relationship between $F(x)$ and x is described in Fig. 2, and the

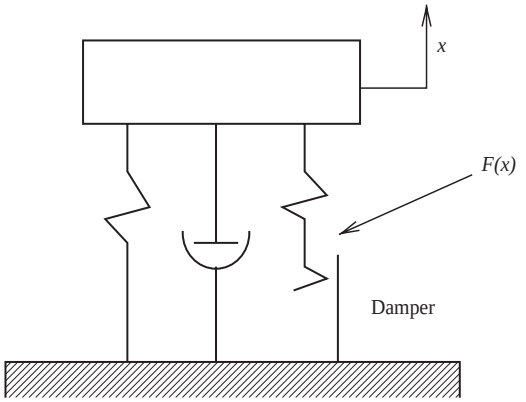

Fig. 1. A nonlinear mechanical system with a hysteretic damper.

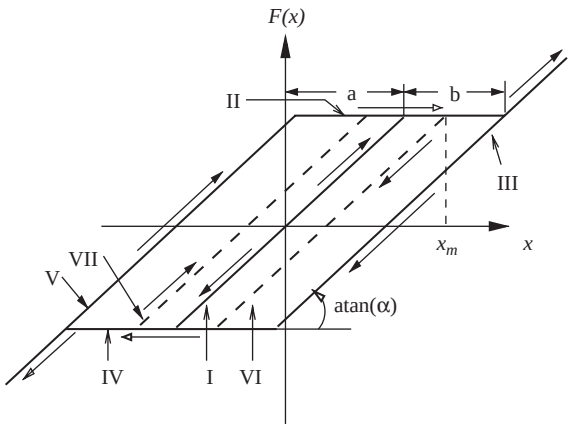

Fig. 2. The hysteretic restoring force.

Table 1
Regular hysteretic force path

Line	$F(x)$	x	$\dot{x}$
I	αx	$(-a, a)$	$(-\infty, \infty)$
II	αa	$[a-b, a+b)$	$[0, \infty)$
III	$\alpha(x-b)$	$(b-a, \infty)$	$(-\infty, \infty)$
IV	$-\alpha a$	$(-a-b, b-a]$	$(-\infty, 0]$
V	$\alpha(x+b)$	$(-\infty, a-b)$	$(-\infty, \infty)$
VI	$\alpha(x-m)$	$(-a+m, a+m)$	$(-\infty, \infty)$
VII	$\alpha(x+m)$	$(-a-m, a-m)$	$(-\infty, \infty)$

mathematical expressions of $F(x)$ with respect to x and $\dot{x}$ are listed in Table 1, where $0<m<b$. Note that the conditions given on the derivative, $\dot{x}$, are not considered by Ding et al. [11]. Also note that path II (or IV) does not change its direction when $x \in [a-b, a)$ (or $x \in (-a, b-a]$). The travelling paths of $F(x)$ follow the following three possible rules (i)–(iii):

(i) I—the central line;
(ii) II → VI → IV → VII → II—the inner loop having two dotted lines (rotating in clock-wise direction); and
(iii) II → III → IV → V → II—the outer loop (rotating in clock-wise direction).

Ding et al. [11] studied the stability and bifurcations of system (1) using the time-averaging method for both autonomous and non-autonomous cases. With the aid of the singularity theory, Wu et al. [12] later investigated the autonomous case to show that the system can have many new bifurcation solutions which were not reported in Ref. [11].

The results obtained by Ding et al. [11] and Wu et al. [12] are based on the assumption that the hysteretic restoring force follows one of the three possible routes described above. As a matter of fact, the results given in Refs. [11,12] confirm that the assumption is correct if no external force exists (i.e., the system is autonomous). However, a careful examination using numerical simulation has revealed that this assumption is no longer true when an external force is applied to the system (i.e., the system becomes non-autonomous). To explain this, consider line II in Fig. 3 (a similar discussion applies to line IV). Note that the significant difference between Figs. 3 and 2 is that Fig. 3 not only has all the line segments of Fig. 2 (lines I–VII which are not shown in Fig. 3) but also two more new line segments (lines VIII and IX), which are not presented in Fig. 2. It has been assumed in Refs. [11,12] that $\dot{x}>0$ for $x \in [a-b, a)$ (i.e., for the first half of the line). Thus, once the restoring force is on this line, it must continue to move until $x \geqslant a$. However, when an external force, $f(t)$, is applied to the system, the characteristics of the restoring force may be changed since the velocity of the motion can become zero even if $x \in [a-b, a)$, implying that the restoring force cannot move further along line II and must change its direction. Such a point is called the *critical turning point*, and we call the associated irregular behavior the *critical phenomenon*. For example, as shown in Fig. 3, $\dot{x}=0$ at point C_1 on line II (and C_2 on line IV) where the restoring force must change its direction and turn to line VIII. Further, note that a large difference occurs on line VIII. In the autonomous case, the region where line VIII is located has

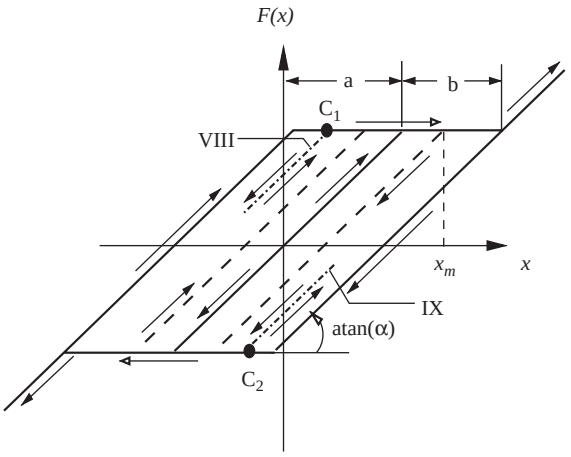

Fig. 3. Hysteretic restoring force under the influence of external forcing.

line VII (see Fig. 2), along which the restoring force continuously moves from line IV to line II, i.e., the moving direction remains upward. In other words, the sign of $\dot{x}$ remains positive on line VII. For the non-autonomous case, however, the restoring force is moving downward along line VIII, which is in the direction opposite to that for the autonomous case. Moreover, it may stop anywhere (at a point where $\dot{x} = 0$) within the region and return to line II, as shown in Fig. 3. Similar possibilities can occur on line IV and the interior region where line VI is located. It has been found that the occurrence of the critical phenomena looks "random". That is, it can occur anywhere in the interior of the domain, in particular, associated with transient vibrations. Naturally, we have assumed that the slopes of the critical lines (e.g., lines VIII and IX) have the same slope, α. In other words, the local natural property of the hysteretic damper remains unchanged under the external excitement.

3. The effect of external force

External forcing plays a very important role in the study of non-autonomous dynamical systems. The dynamical behavior of such a system like instability and bifurcations is much more complicated than that of a system without external force (autonomous system). In the previous section, we have discussed the effect of external forcing on the dynamical behavior of system (1). In this section, numerical simulation results are presented to demonstrate that the effect of the external force is crucial. We consider the variation of the amplitude of the external force, K (starting from small values), to monitor the effect of the external force, while the frequency, Ω, is fixed as $\Omega = 0.5$.

In addition to the two parameters, K and Ω, the values of other parameters of the system, a, b, α and β, are chosen as

$$a = 0.056, \quad b = 0.2, \quad \alpha = 0.125, \quad \beta = 0.171. \tag{2}$$

When $K = 0$ (no external force), the dynamical solutions of hysteretic system are simple periodic motions (limit cycles). Although the amplitudes of the periodic solutions can vary with respect to different initial conditions, as reported in Ref. [14] (see Fig. 4), no other complex dynamical behavior (such as quasi-periodic solutions or chaos) has been observed. In particular, the travelling paths for the hysteretic force clearly follow the regular bilinear path defined in the previous section (see the possible paths I, II and III shown in Fig. 2).

When K is varied from 0 to a very small positive number, the effect of the external force is negligible. For example, when $K = 0.01$, the phase portraits of the trajectories are almost identical to that shown in Fig. 4 for the autonomous case. A further increase of the external force shows the crucial effect of the external force on the dynamical behavior—the periodic solutions become

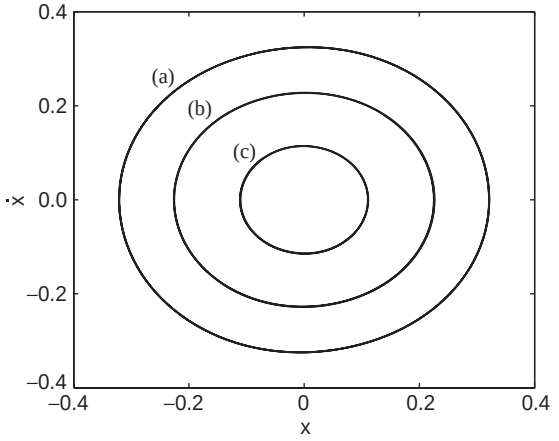

Fig. 4. Phase portraits for $K = 0$ (no external force) with the initial conditions: (a) $x = 0.36$, $\dot{x} = 0.005$; (b) $x = 0.20$, $\dot{x} = 0.005$; and (c) $x = 0.026$, $\dot{x} = 0.005$.

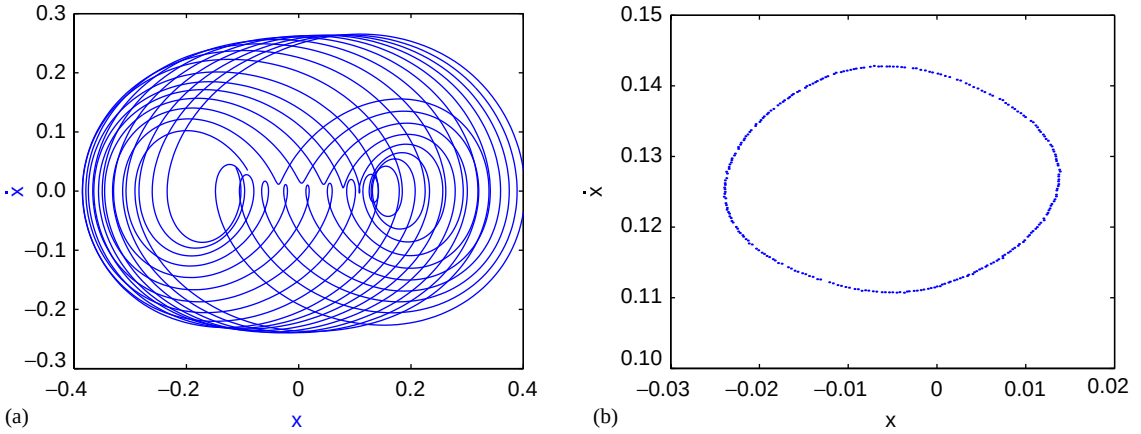

Fig. 5. Quasi-periodic solution for $K = 0.2$: (a) phase portrait, (b) Poincaré map.

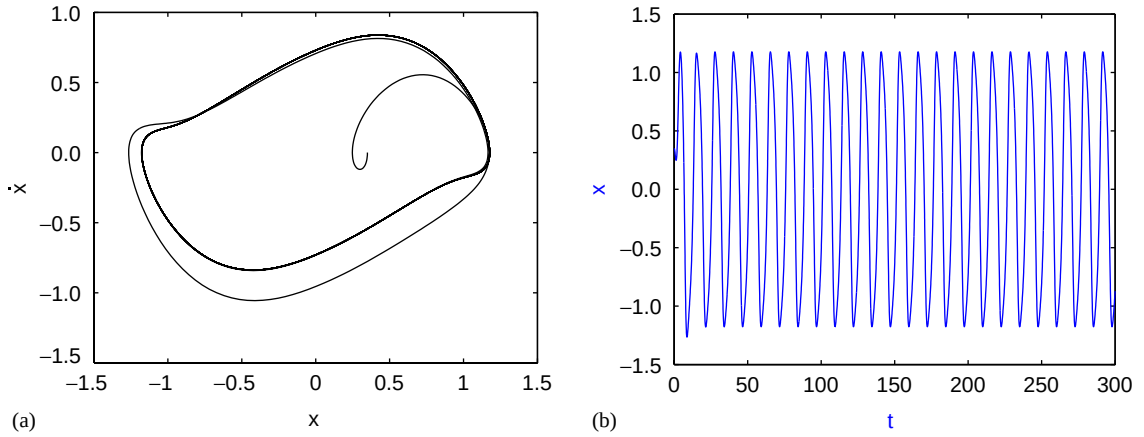

Fig. 6. Periodic solution for $K = 1.0$: (a) phase portrait, (b) time history.

quasi-periodic. For instance, when $K = 0.2$, system (1) exhibits quasi-periodic motions, as shown in Fig. 5. We may apply the concept of mode competition developed by Yao et al. [16] to explain this phenomenon as follows. System (1) can be considered as a dynamical system with two modes; one of them is characterized by the internal mode with frequency $\omega \approx 1$ and the external mode with frequency Ω. The two modes represent two different motions which are either in competition or one dominates the other. When one mode dominates the other, the motion is simply periodic since the system basically has only one frequency. However, when the two modes are in competition (i.e., neither one dominates the other), the motion becomes complex because there exists interaction between the two different modes. For system (1), when $K \approx 0$, the external mode is dominated by the internal mode, and thus the motion is periodic. However, when K takes a medium value, the two modes are in competition and the motion becomes quasi-periodic since the motion contains more than one frequency.

As the amplitude of the external force increases further, the quasi-periodic motions return to periodic, as observed in most forcing vibrations. This is because the external mode now dominates the internal mode and the periodic solutions are mainly characterized by the external mode with frequency Ω. The transition from quasi-periodic to periodic motions occurs at the critical value of $K \approx 0.4$. Once the motion becomes periodic, the path of the $F(x)$ returns to regular. Such an example is depicted in Fig. 6 for $K = 1.0$, showing a large (global) limit cycle. It should be pointed out that this large limit cycle (see Fig. 6) is quite different compared to the small ones (see Fig. 4).

A summary of the above discussions and results indicates that adding an external force to a hysteretic system can complicate the dynamics of the system, and the bifurcation analysis becomes even more involved.

4. Critical phenomena

In this section, we turn to illustration of the critical phenomena exhibited in the hysteretic system (1). We shall show that for certain cases, when external force is present, the regular

hysteretic force paths become irregular, which was not described in the original hysteretic model [11]. Therefore, some dynamical behavior of the mechanical system (1) studied by Ding et al. [11] was not correctly described. The *critical phenomena* due to the external forcing have been briefly discussed by Chen et al. [14]. In this section, we shall give a more detailed analysis.

In the previous section, we have shown that the hysteretic system with external forcing can exhibit more complicated dynamical behavior. The autonomous system (without external force) can only exhibit periodic solutions (although it may have multiple periodic solutions which depend on the initial condition), while the non-autonomous system (with external forcing) can have quasi-periodic as well as periodic motions. Moreover, subharmonic and super-harmonic resonances have been observed in such a non-autonomous system. It has been reported that the autonomous system does not have critical phenomena, while the non-autonomous system exhibits the critical phenomena when the system has quasi-periodic solutions [14]. Here, we shall further show that the critical phenomena also exist in subharmonic or super-harmonic resonant solutions. The critical phenomena persist even when a steady state is reached.

For the numerical simulation, we fix the values of the parameters, a, b, α, K and β, but change Ω. For a consistent comparison with the results presented by Ding et al. [11], we select the same values used in Ref. [11], given by

$$K = 1.0, \quad a = 0.3, \quad b = 0.8, \quad \alpha = 1.0, \quad \text{and} \quad \beta = 0.5. \tag{3}$$

A detailed dynamical analysis was carried out by Ding et al. [11] using the average method, but no critical phenomenon was reported. Here, we use extensive numerical simulations, with the variation of Ω and the plotting of the hysteretic force paths, to identify the critical phenomena. By inspecting the hysteretic force paths, we found that the critical phenomena may exist in different dynamical motions. In the following, we particularly consider subharmonic and super-harmonic motions.

4.1. Subharmonic motion

In the subharmonic resonant case, we vary Ω from 0.1 (Hz) to 4.0 (Hz) continuously, and then plot the hysteretic force paths for various parameter values. Numerical simulation results show that the dynamical motions can be quasi-periodic, subharmonic and super-harmonic in various orders. An interesting phenomenon (the critical phenomenon) occurs in the subharmonic resonance when Ω is increased to 1.87. When the motion reaches its steady state for this value of Ω, the phase portrait and restoring force path are shown in Fig. 7. The hysteretic path seems regular, but it is actually not. On path VI, the restoring force path goes downward from point 1 to point 2, as shown in Fig. 7(b). The velocity of the mass decreases from positive values to 0 somewhere on the path (at point 2); thus, the restoring force stops moving, changes its direction and goes up (from point 2 to point 1). When it reaches path II (at point 1), the velocity becomes 0 again; thus, it goes downward once more (from point 1 to point 3), and this time it continuously moves downward to path IV and turn left. This phenomenon and associated path are not described in the hysteretic function of the original system. As we further increase the values of Ω to reach 1.93, the critical phenomenon disappears.

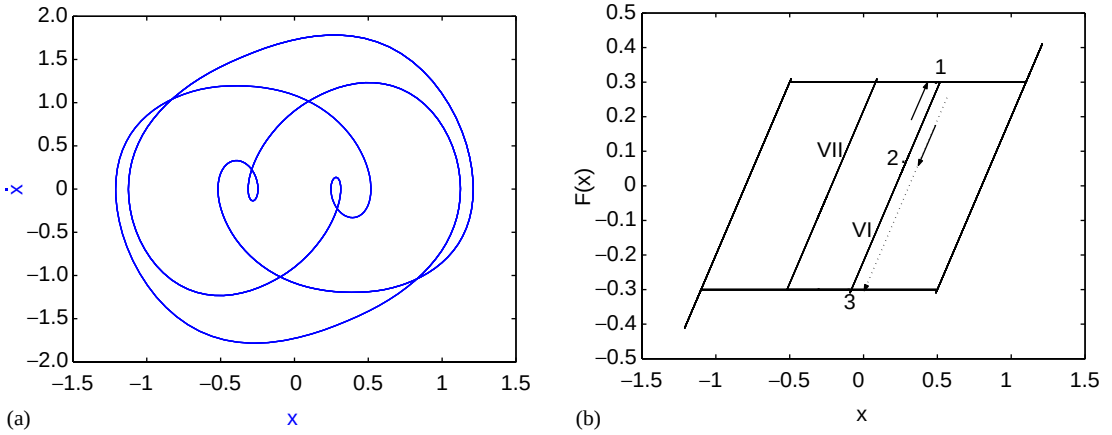

Fig. 7. Subharmonic case for $\Omega = 1.87$: (a) phase portrait, (b) restoring force path.

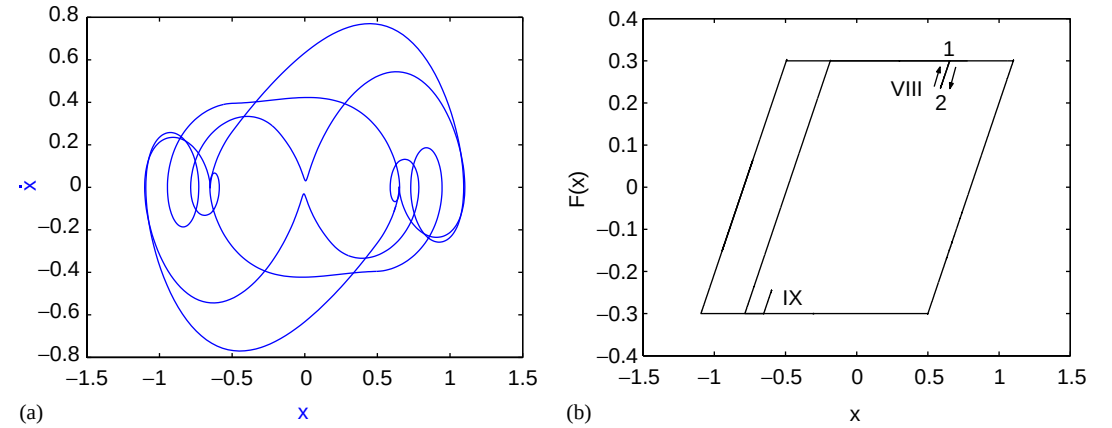

Fig. 8. Super-harmonic case for $\Omega = 0.32$: (a) phase portrait, (b) restoring force path.

4.2. *Super-harmonic motion*

When $\Omega \approx 0.32$, the super-harmonic resonant motions are observed, as depicted in Fig. 8. The critical phenomena are clearly seen when the motion reaches its steady state. In this case, the irregular hysteretic path is obvious. At point 1, the velocity is zero; thus, the hysteretic force goes downward to point 2. The hysteretic force stops at point 2 in the middle of path VIII or IX (see Fig. 8(b)) and then returns to point 1 to take the regular path, as described in Fig. 8(b). This finding reveals that the description of the model given by Ding et al. [11] is incomplete. A revised hysteretic force model shown in Fig. 3 should be used to correctly reflect the change of the characteristics of the hysteretic system when external forcing is present.

4.3. Spectral analysis

In this subsection, we will try to give an explanation of the critical phenomenon, by using the concept of mode competition [16]. It will be shown that a necessary condition for the hysteretic system to exhibit the critical phenomenon is that the system has at least two modes, which are in competition (i.e., none of the two modes dominates the other). Spectral analysis will be used to verify the above conclusion.

We shall consider three cases: super-harmonic oscillation, subharmonic oscillation and quasi-periodic motion. Both situations, with and without the critical phenomenon, are considered. Numerical simulation results for phase portraits and spectra are depicted in Figs. 9–14, where Figs. 9 and 10 show the comparison between the cases with and without the critical phenomenon

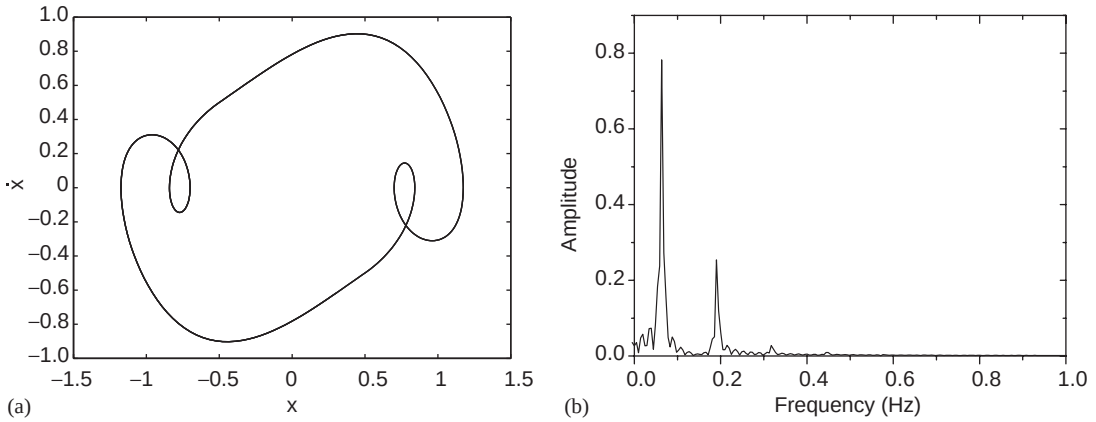

Fig. 9. Super-harmonic case for $K = 1.0$ and $\Omega = 0.4$: (a) phase portrait, (b) spectral diagram.

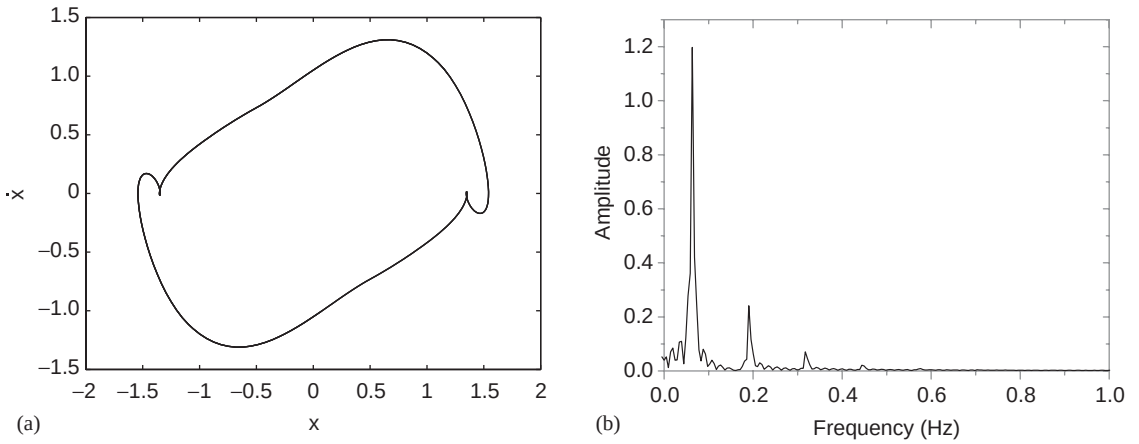

Fig. 10. Super-harmonic case for $K = 2.0$ and $\Omega = 0.4$: (a) phase portrait, (b) spectral diagram.

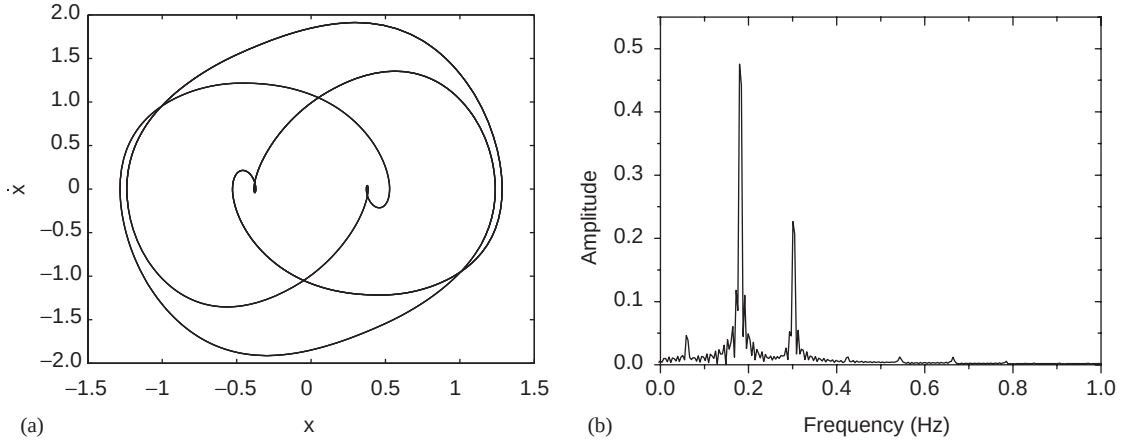

Fig. 11. Subharmonic case for $K = 1.0$ and $\Omega = 1.90$: (a) phase portrait, (b) spectral diagram.

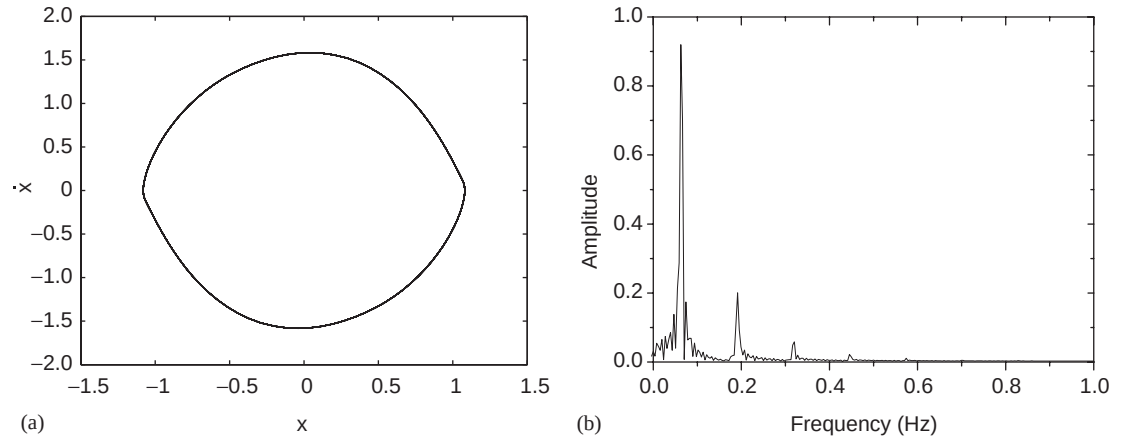

Fig. 12. Subharmonic case for $K = 1.0$ and $\Omega = 3.35$: (a) phase portrait, (b) spectral diagram.

for super-harmonic motions, Figs. 11 and 12 for subharmonic motions, and Figs. 13 and 14 for quasi-periodic motions, respectively.

First, it is noted from Figs. 9, 11 and 13 that all the critical phenomena occurring in the three cases must be associated with at least two frequencies: one of which is the external frequency and the other is the system's internal natural frequency, as shown by the spectra given in Figs. 9(b), 11(b) and 13(b). In fact, with numerical simulations it has been observed that two frequencies always exist in all the critical phenomena reported in this paper for system (1). This seems to show that a necessary condition for the existence of critical phenomena is that system (1) has at least two frequencies (modes).

Then a question arises: is this necessary condition also sufficient? In other words, if there exist two frequencies (modes), would the motion appear critical? Unfortunately, the answer is no. As a

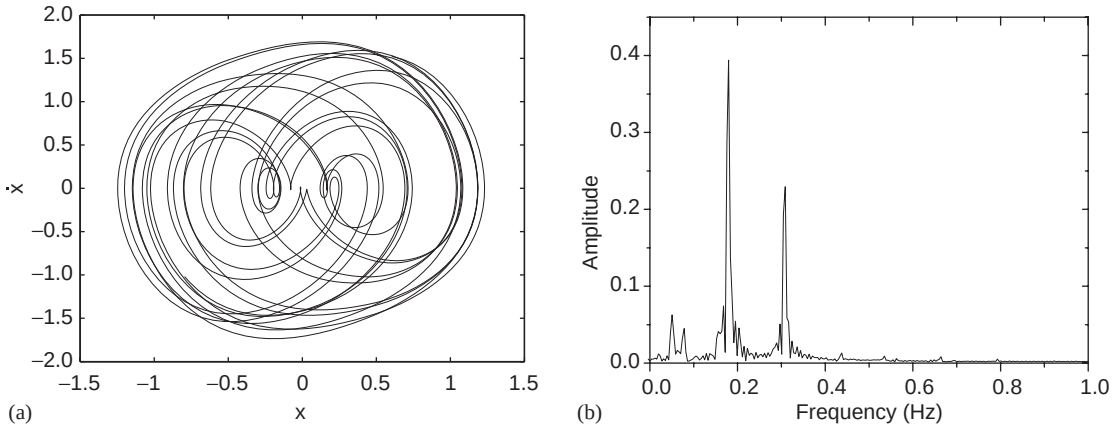

Fig. 13. Quasi-periodic case for $K = 1.0$ and $\Omega = 1.93$: (a) phase portrait, (b) spectral diagram.

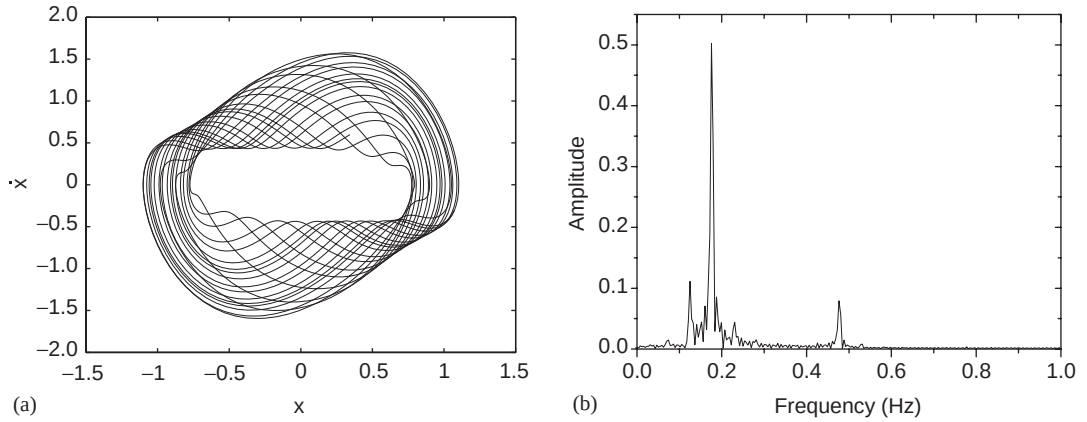

Fig. 14. Quasi-periodic case for $K = 1.0$ and $\Omega = 3.0$: (a) phase portrait, (b) spectral diagram.

matter of fact, we have found many cases in which there exist two frequencies (modes), but they are not associated with the critical phenomenon. Three such cases, one for super-harmonic motion, one for subharmonic motion and one for quasi-periodic motion, are shown in Figs. 10, 12 and 14, respectively. Then one would further ask: what is the difference between the critical and non-critical cases, or what is the particular characteristics of the critical phenomena? By comparing the spectra of the three cases given in Figs. 9(b) and 10(b), 11(b) and 12(b), and 13(b) and 14(b), we observe that when a critical phenomenon occurs, the amplitudes of the two modes (associated with the two frequencies) are relatively comparable, while in the case without the critical phenomenon, one mode dominates the other.

A summary of the discussions given in this sub-section suggests that a necessary condition leading to the critical phenomenon is: there should exist at least two competitive modes in the system.

5. Chaos control using hysteretic force

In the past two decades, there has been rapidly growing interest in bifurcation and chaos control. Such bifurcation and chaos control techniques have been widely applied to solve physical and engineering problems (e.g., see Refs. [17–19]). In this section, we shall show that the hysteretic force can be used to suppress the chaotic motions, which are generated by the simple driven van der Pol oscillator. The driven van der Pol system without hysteretic force has been widely studied, providing a prototype model which exhibits a large variety of nonlinear phenomena such as periodically disturbed limit cycles, mode-locking and period doubling leading to chaos. Parlitz et al. [20] studied the mode-locking phenomena and period-doubling cascades of the forced van der Pol system. A more complete dynamical analysis was given by Mettin et al. [21] which also showed chaotic motions in the driven van der Pol system under both subharmonic and super-harmonic resonances. For a consistent comparison, we shall report our results here for the influence of the hysteretic force on the chaotic motions of the driven van der Pol system in two cases: subharmonic resonance and super-harmonic resonance. We fix the values of a and b as

$$a = 0.3, \quad \text{and} \quad b = 0.8. \tag{4}$$

5.1. Subharmonic resonant case

The dynamics of the driven van der Pol system is governed by the equation

$$\ddot{z} + d\,(z^2 - 1)\,\dot{z} + z = a\,\cos\omega t, \tag{5}$$

which has been discussed in detail by Mettin et al. [21]. The system undergoes bifurcations from period-doubling to chaos for certain parameter values. For example, for $a = 15$ and $d = 3$, when ω is changed from 3.96 to 3.98, the motions of system (5) change from period-4 to chaos via period-doubling [21].

In order to transform system (5) to the form of our Eq. (1), introducing the scaling $z = \xi x$ into system (5) yields

$$\ddot{x} + d(\xi^2 x^2 - 1)\dot{x} + x = \frac{a}{\xi}\cos\omega t. \tag{6}$$

Then, let $d = \beta$, $d\xi^2 = 1$ under which system (6) can be written as

$$\ddot{x} + (x^2 - \beta)\dot{x} + x = a\sqrt{\beta}\,\cos\omega t. \tag{7}$$

Further, let $K = a\sqrt{\beta}$; system (7) finally becomes system (1) without hysteretic force. Thus, if we choose $\beta = d = 3$, $K = a\sqrt{\beta} = 15\sqrt{3}$, system (1) (without hysteretic force) undergoes bifurcations from periodic doubling to chaos as ω is varied from 3.96 to 3.98. The phase portraits and Poincaré maps for the bifurcations leading to chaos, obtained from our computer simulations, are shown in Figs. 15–17.

Next, we fix $\omega = 3.98$ and increase the value of α (the coefficient in the hysteretic force; see Table 1) to monitor the influence of hysteretic force. As we see from the computer simulation results, shown in Fig. 18, the system remains chaotic when α is small. However, when α is increased to a certain value ($\alpha \geqslant 0.2$ for this case), the chaos is suppressed and the system is

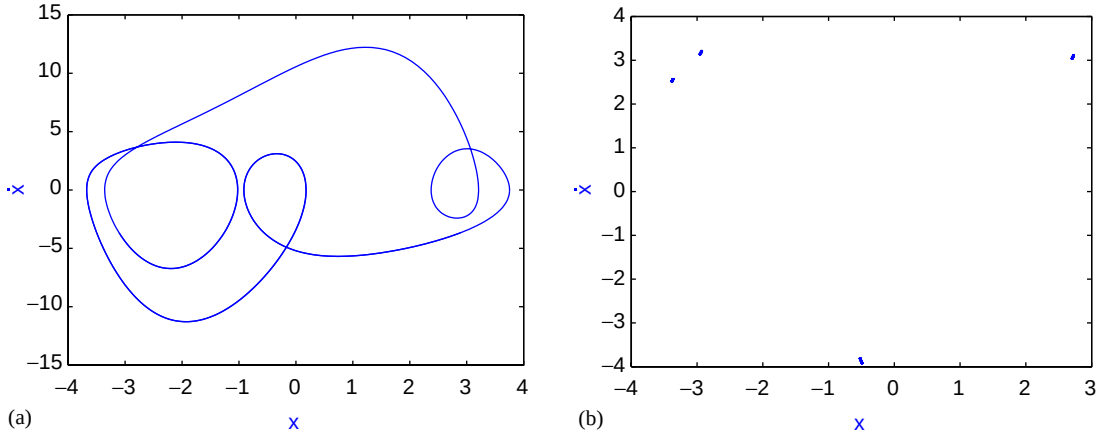

Fig. 15. Simulation results for $\omega = 3.96$: (a) phase portrait, (b) Poincaré section.

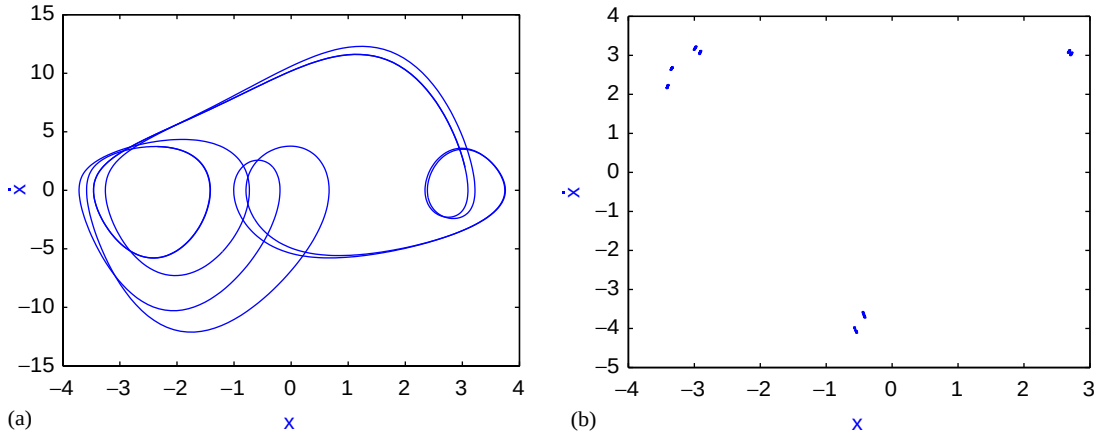

Fig. 16. Simulation results for $\omega = 3.97$: (a) phase portrait, (b) Poincaré section.

returned to the stable periodic motion; see an example shown in Fig. 19(a) in which $\alpha = 1.5$. Further increase of the amplitude of the hysteretic force can reduce the period of the stable solution, as depicted in Fig. 19(b) where the motion is a period-1 solution when $\alpha = 10$.

To our knowledge, this new finding described above has not been reported in the literature. This suggests a new method for controlling chaos using the hysteretic force. This simple chaos control approach may enhance new applications in the field of chaos control. Certainly, in the absence of the hysteretic force, one can adjust the amplitude, the frequency, or both of the external force to control chaos. However, in practice, the amplitude of the external force might not be able to reach very large values due to physical constraints, or it might not guarantee to clear away small and medium values of the amplitude; then, one must consider some other control strategies. Using a hysteretic force is a new alternative. For example, as illustrated in the previous section, one may use a large enough amplitude of the hysteretic force to suppress chaos.

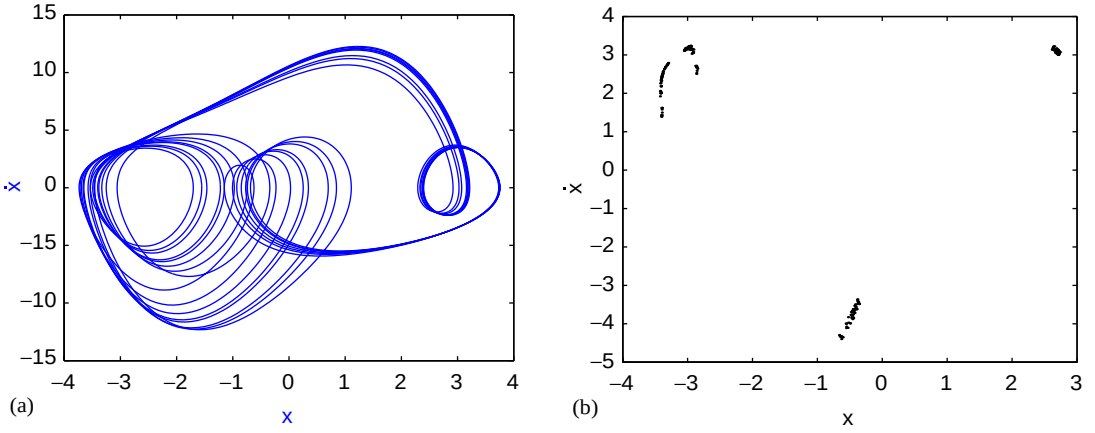

Fig. 17. Simulation results for $\omega = 3.98$: (a) phase portrait, (b) Poincaré section.

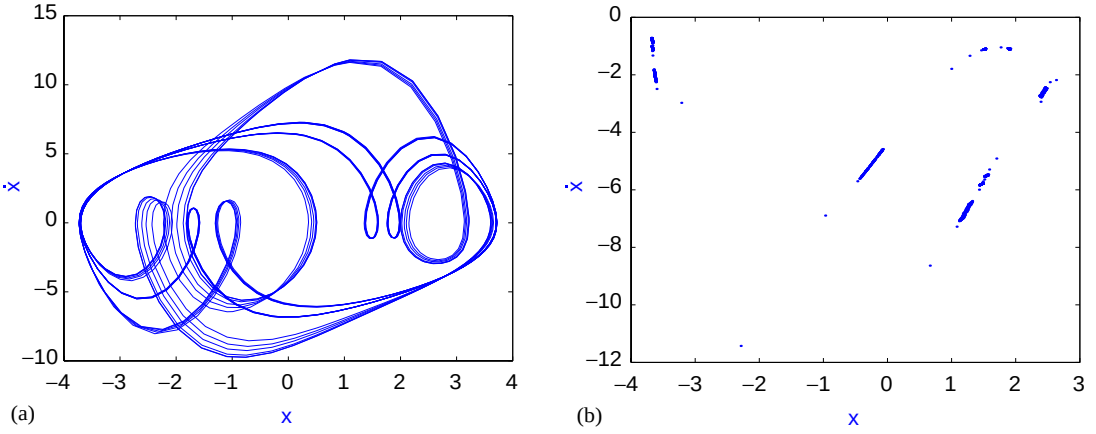

Fig. 18. Simulation results for $\omega = 3.98$ and $\alpha = 0.1$: (a) phase portrait, (b) Poincaré section.

Moreover, this new approach does not need to apply extra force since the hysteretic force is an inherent characteristic of the material. Another point that should be noted is: varying the amplitude of an external force to controlling chaos means changing the input of energy to the system. (Applying an external force with larger amplitude inputs more energy to the system.) However, using a hysteretic force to suppress chaos does not change the energy of the system because it uses the characteristics of the material.

Certainly, in the case of using external force to control chaos, one can also adjust the frequency, Ω. To demonstrate the advantages of using the hysteretic force over using the frequency modulation of an external force, we have compared these two methods and found the following facts.

- Chaos control by varying the frequency of the external force is much more sensitive than that of using the hysteretic force. A bifurcation diagram under the variation of the frequency, ω, is

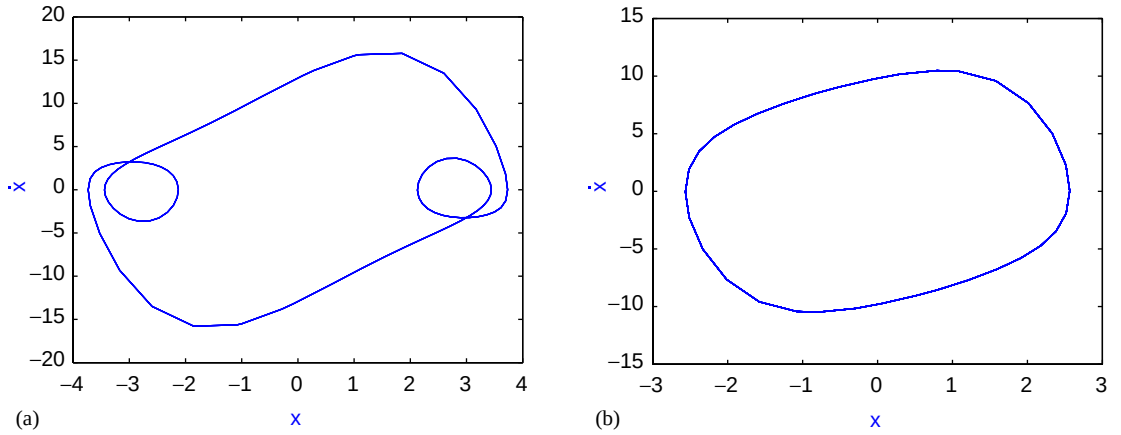

Fig. 19. Phase portraits for $\omega = 3.98$ when (a) $\alpha = 1.5$, (b) $\alpha = 10.0$.

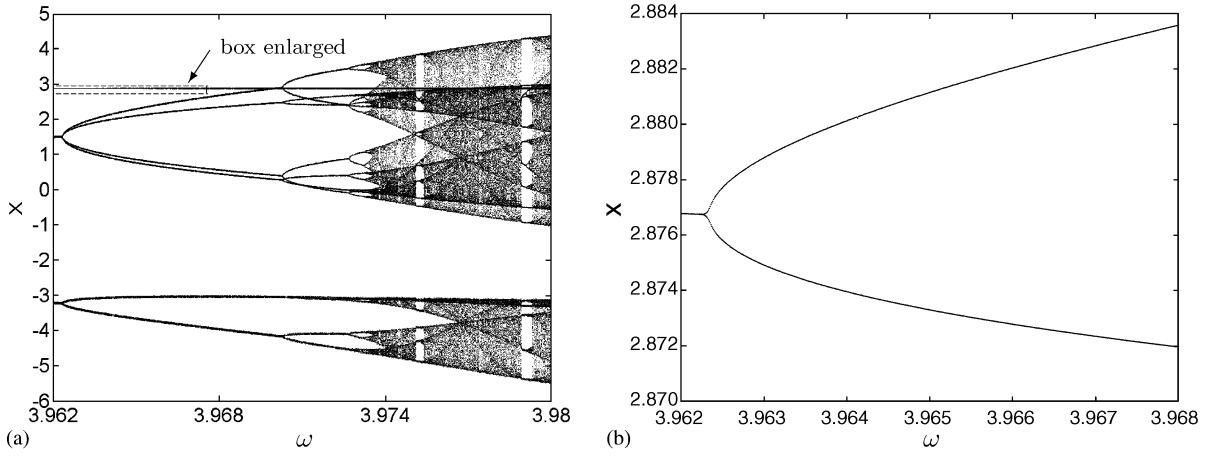

Fig. 20. Bifurcation diagram of system (1) when $F = 0$ for $\omega \in [3.962, 3.98]$: (a) the complete bifurcation diagram; and (b) a zoomed in part of the box in part (a).

shown in Fig. 20 for the case without the hysteretic force. This figure is obtained by taking the intersection points of trajectories on a Poincaré section. The bifurcation diagram given in Fig. 20(a) clearly indicates that the system with external force can have very rich dynamic behavior such as periodic orbits, double period leading to chaos, windows having periodic motions. This figure reminds one of the similarity to the well-known logistic map. The left top part of Fig. 20(a) seems like a "line". But in fact, this "line" has a bifurcation around the point $\omega = 3.9623$ at which a lowest order bifurcation occurs. This is zoomed in Fig. 20(b). When the hysteretic force reaches certain values, the system can have periodic solutions for any ω between 3.96 and 3.98. For example, if we choose $\alpha = 10$, then for any values of the frequency, say, $\omega \in (3.92, 3.98)$, no chaos exists. Fig. 21 shows a case when $\omega = 3.92$ and $\alpha = 10$, giving rise to a stable limit cycle.

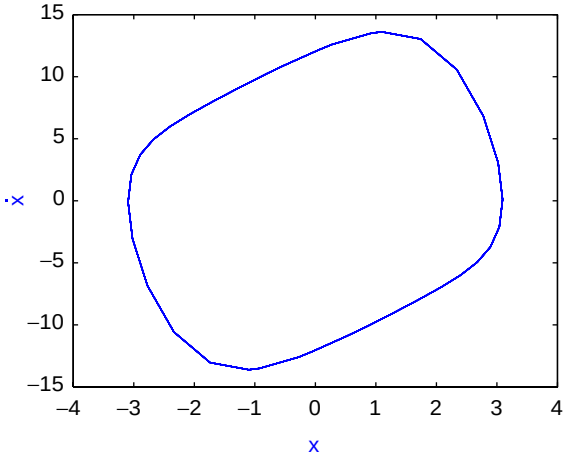

Fig. 21. Phase portrait when $\omega = 3.92$ and $\alpha = 10.0$.

- Using hysteretic force, we can obtain stable solutions which cannot be obtained by controlling the frequency of the external force. For example, when $\alpha = 10$, we can obtain a period-1 solution by using hysteretic force control (see Fig. 19(b)).
- The chaos control using hysteretic force is easy to realize in practice. For example, for the set of parameter values used above, it has been shown by Mitten [21] that the motions of the van der Pol system are chaotic for a large range of frequency values. Thus, in order to use the frequency of an external force to transfer chaos to a stable periodic motion, one needs to search the whole domain of ω where the system has stable periodic solutions, which is very time-consuming. However, by using the hysteretic force control, we can easily suppress the chaos even with a relatively small hysteretic force.

5.2. *Super-harmonic resonant case*

Under the choice of the parameter values

$$\beta = 1.0, \quad K = 1.035 \quad \text{and} \quad \omega = \tfrac{1}{2.14823}, \tag{8}$$

the driven van der Pol system without hysteretic force exhibits chaos [8]. The Poincaré map of the trajectories of the system is shown in Fig. 22. The Lyapunov exponent [22] for this case is obtained as $\lambda = 0.7$, confirming that the motion is chaotic.

Similar to the discussions given for the subharmonic resonant case, we vary the value of α to monitor the influence of hysteretic force on the motions of the van der Pol system. The numerical study shows that when α is very small (e.g., $\alpha = 0.001$), the system reserves the dynamical characteristics of the van der Pol system (see Fig. 23). When α is increased to $\alpha = 0.01$, the chaos disappears and the motion becomes a period-5 solution, as shown in Fig. 24. Continuing the increase of α to, say, $\alpha = 0.1$ yields a period-2 solution (see Fig. 25 where both phase portrait and

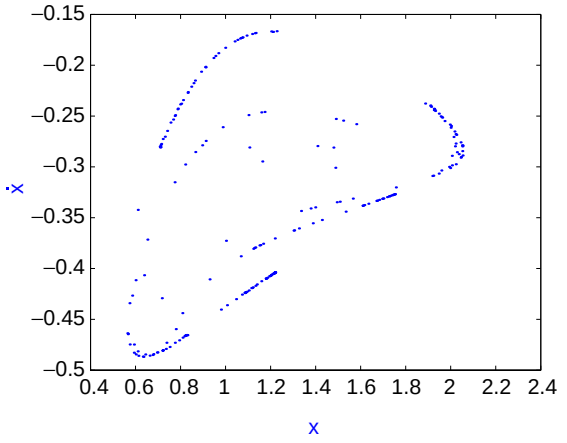

Fig. 22. Poincaré section of a chaotic attractor.

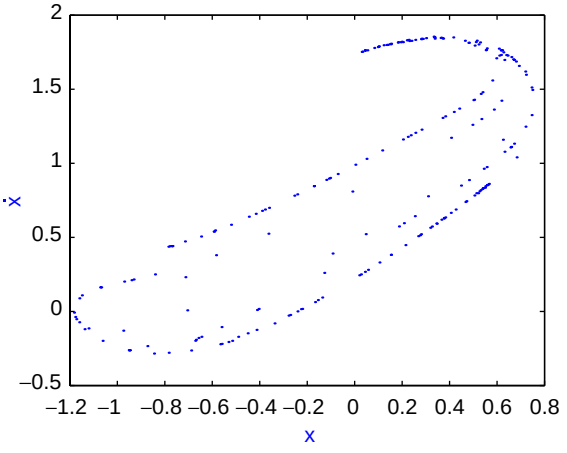

Fig. 23. Poincaré section when $\alpha = 0.001$.

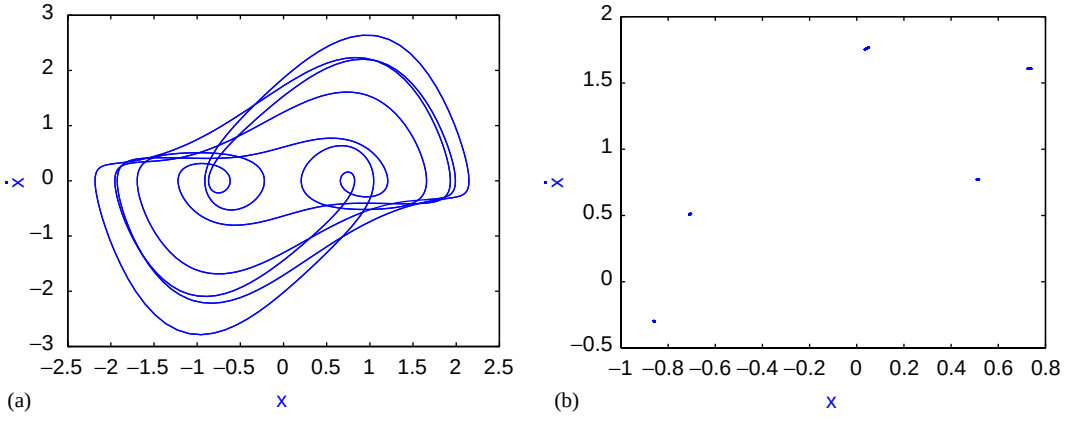

Fig. 24. Simulation results for $\alpha = 0.01$: (a) phase portrait, (b) Poincaré section.

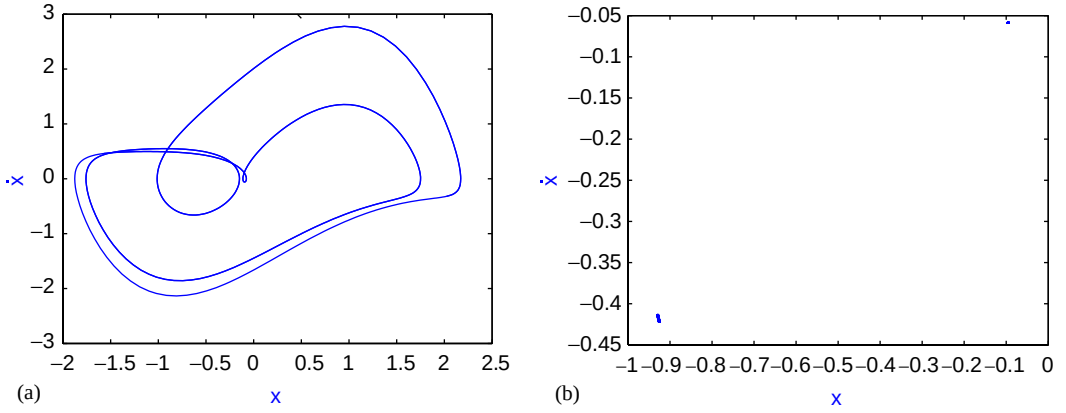

Fig. 25. Simulation results for $\alpha = 0.1$: (a) phase portrait, and (b) Poincaré section.

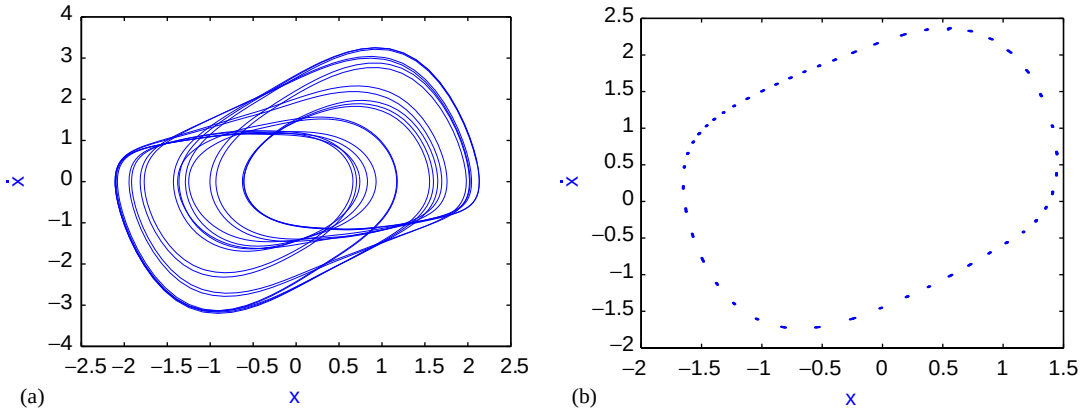

Fig. 26. Simulation results for $\alpha = 1.5$: (a) phase portrait, (b) Poincaré section.

Poincaré map are presented). A further increase of α can generate quasi-periodic motions. Such an example is shown in Fig. 26 in which $\alpha = 1.5$.

6. Conclusions

A self-excited hysteretic system with external force has been studied. Numerical simulation results show that the description of the hysteretic restoring force used for the original model was not complete. The influence of external force can dramatically change the dynamic behavior of the hysteretic system, where the critical phenomena in hysteretic loop exist in both transition and steady states. A revised hysteretic force path (given in Fig. 3) has been proposed to give better and consistent results with the original model. It has been shown using spectral analysis that the

existence of at least two competitive modes in a hysteretic system is a necessary condition for the system to exhibit the critical phenomenon. Also, it has been found that hysteretic force can be used to suppress chaos, as shown by using the driven van der Pol system. We hope that this study will raise interest in the study of the influence of external force on the dynamical behavior of hysteretic systems as well as the application of hysteretic force in controlling chaos. Experimental work is needed to verify the results obtained in this paper.

Acknowledgements

The support received from the Natural Science and Engineering Research Council of Canada (NSERC No. R2686A02), the National Natural Science Foundation of China (NSFC No. 10102014) and OGSST (Ontario Graduate Scholarship of Science and Technology) is gratefully acknowledged.

References

[1] P. Krejci, Reliable solution to the problem of periodic oscillations of an elastoplastic beam, *International Journal of Nonlinear Mechanics* 37 (2002) 1337–1349.
[2] F. Vestroni, M. Noori, Hysteresis in mechanical systems—modeling and dynamic response, *International Journal of Nonlinear Mechanics* 37 (2002) 1261–1262.
[3] S. Otani, Hysteresis models of reinforced concrete for earthquake response analysis, *Proceedings of the Eighth World Conference on Earthquake Engineering*, San Francisco, 1984.
[4] D. Feng, T. Miyama, T. Torii, S. Yoshida, M. Ikenaga, I. Shimoda, A new analytical model for the lead rubber bearing, *Proceedings of the Twelfth World Conference on Earthquake Engineering*, Auckland, New Zealand, 2000.
[5] R. Gorbet, K. Morris, D. Wang, Passivity-based stability and control of hysteresis in smart actuators, *IEEE Transactions on Control Systems Technology* 9 (2001) 5–16.
[6] S. Seelecke, Modeling the dynamic behavior of shape memory alloys, *International Journal of Nonlinear Mechanics* 37 (2002) 1363–1374.
[7] A. Masuda, M. Noori, Optimization of hysteretic characteristics of damping devices based on pseudoelastic shape memory alloys, *International Journal of Nonlinear Mechanics* 37 (2002) 1375–1386.
[8] P. Lehmann, F. Stauffer, C. Hinz, O. Dury, H. Flühler, Effect of hysteresis on water flow in a sand column with a fluctuating capillary fringe, *Journal of Contaminant Hydrology* 33 (1998) 81–100.
[9] R. Pyke, Non-linear soil models for irregular cyclic loadings, *Journal of the Geotechnical Engineering Division* 105 (1979) 715–726.
[10] W. Lacarbonara, F. Vestroni, Nonclassical responses of oscillators with hysteresis, *Nonlinear Dynamics* 32 (2003) 235–258.
[11] Q. Ding, A.Y.T. Leung, J.E. Cooper, Dynamic analysis of a self-excited hysteretic system, *Journal of Sound and Vibration* 245 (2001) 151–164.
[12] Z. Wu, K. Wang, P. Yu, Bifurcation analysis on a self-excited hysteretic system, *International Journal of Bifurcation and Chaos* 14 (2004) 2825–2842.
[13] E.H. Dowell, *Aeroelasticity of Plates and Shells*, Noordhoff, Leyden, 1975.
[14] Z. Chen, Z. Wu, P. Yu, Analysis on critical phenomena of a self-excited hysteretic system, *Proceedings of the 2003 ASME International Mechanical Engineering Congress and Exposition*, ASME DE-Vol. 2, November 15–21, Washington, DC, 2003.
[15] A.Y.T. Leung, T.C. Fung, Analytical solutions of elasto-plastic systems, *Journal of Sound and Vibration* 142 (1990) 175–182.

[16] W. Yu, P. Yu, C. Essex, Estimation of chaotic parameter regimes via generalized competitive mode approach, *Communications in Nonlinear Science and Numerical Simulation* 7 (2002) 197–205.
[17] G. Chen, J.L. Moiola, H.O. Wang, Bifurcation control: theories, methods, and applications, *International Journal of Bifurcation and Chaos* 10 (2000) 511–548.
[18] H.O. Wang, E.G. Abed, Bifurcation control of a chaotic system, *Automatica* 31 (1995) 1213–1226.
[19] P. Yu, G. Chen, Hopf bifurcation control using nonlinear feedback with polynomial functions, *International Journal of Bifurcations and Chaos* 14 (2004) 1683–1704.
[20] U. Parlitz, W. Lauterborn, Period-doubling cascades and Devil's staircases of the driven van der Pol oscillator, *Physical Review A* 36 (1987) 1428–1434.
[21] Mettin, U. Parlitz, W. Lauterborn, Bifurcation structure of the driven van der Pol oscillator, *International Journal of Bifurcation and Chaos* 3 (1993) 1529–1555.
[22] A. Wolf, J.B. Swift, H.L. Swinney, J.A. Vastano, Determining Lyapunov exponents from a time series, *Physica D* 16 (1985) 285–317.